An Excited State Density Functional Theory Study of the Rhodopsin Chromophore

C. Molteni,* I. Frank,† and M. Parrinello

Contribution from the Max-Planck-Institut für Festkörperforschung, Heisenbergstrasse 1, D-70569 Stuttgart, Germany

Received October 20, 1998. Revised Manuscript Received October 4, 1999

Abstract: Using a recently developed scheme for performing, within density functional theory, molecular dynamics and geometry optimization for fairly large systems in the first excited singlet state, we have studied the structure and energy changes that the rhodopsin chromophore undergoes during the photoisomerization from *11-cis* to *all-trans*. We discuss the effects of relevant parts of the protein environment close to the chromophore on the isomerization barrier and on the chromophore structure.

The primary event of vision is believed to involve the photoisomerization of the chromophore of rhodopsin, the photosensitive protein of the retina consisting of seven α helices, from its *11-cis* to its *all-trans* isomer.[1−4] This is an extremely fast and efficient process, essentially barrierless, which is completed within 200 fs with a quantum yield of 0.67; it is then followed by a series of chemical reactions that culminate in the stimulation of the optical nerve.[5,6] A sketch of the rhodopsin chromophore, i.e. retinal covalently bound to the apoprotein opsin *via* a protonated Schiff base, is shown in Figure 1. The chromophore of rhodopsin is very similar to that of bacteriorhodopsin, a protein found in the purple membrane of the archaeon *halobacterium salinarium*, which isomerizes from *all-trans* to *13-cis* and which acts as a light-driven proton pump. Rhodopsin[5−11] and bacteriorhodopsin[12−21] have been investigated thoroughly. Both compounds are trans-membrane proteins, difficult to crystallize. Because of the low quality of the crystals, the resolution of the available X-ray structures is very low; this is especially true for rhodopsin. Computed protein models consistent with the experimental data can be taken, with obvious caution, as approximate reference structures.[22] Calculations include force-field,[23−27] semiempirical,[29−43] and *ab initio* methods,[27,28,43−62] and also combined classical/quantum mechanical simulations,[28,31] applied to more or less complex

* Address correspondance to this author at Theory of Condensed Matter group, Cavendish Laboratory, University of Cambridge, Madingley Road, Cambridge CB3 0HE, Great Britain.

† Present address: Institut für Physikalische Chemie, Butenandtstrasse 5-13, Haus E, 81377 München, Germany.

(1) Birge, R. R. *Biochim. Biophys. Acta* **1990**, *92*, 7179−7195.
(2) Birge, R. R. *Annu. Rev. Biophys. Bioeng.* **1981**, *74*, 5669−5678.
(3) Hargrave, P. A.; McDowell, J. H. *Int. Rev. Cytol. B* **1992**, 49−97.
(4) Wald, G. *Nature* **1968**, *219*, 800−807.
(5) Schoenlein, R. W.; Peteanu L. A.; Mathies, R. A.; Shank, C. V. *Science* **1991**, *254*, 412−415.
(6) Peteanu L. A.; Schoenlein, R. W.; Wang, Q.; Mathies, R. A.; Shank, C. V. *Proc. Natl. Acad. Sci. U.S.A.* **1993**, *90*, 11762−11766.
(7) Wang, Q.; Schoenlein R. W.; Peteanu L. A.; Mathies, R. A.; Shank, C. V. *Science* **1994**, *266*, 422−424.
(8) Gärtner, W.; Ternieden, S. J. *Photochem. Photobiol. B Biol.* **1996**, *33*, 83−86.
(9) Koch, D.; Gärtner, W. *Photochem. Photobiol.* **1997**, *65*, 181−184.
(10) Kochendoerfer, G. G.; Mathies, R. A. *J. Phys. Chem.* **1996**, *100*, 14526−14532.
(11) Kandori, H.; Sasabe, H.; Nakanisi, K.; Yoshizawa, T.; Mizukami, T.; Shichida, Y. *J. Am. Chem. Soc.* **1996**, *118*, 1002−1005.
(12) Pebay-Peyroula, E.; Rummel. G.; Rosenbusch, J. P.; Landau, E. M. *Science* **1997**, *277*, 1676−1681.
(13) Oesterhelt, D.; Stoeckenius, W. *Proc. Natl. Acad. Sci. U.S.A.* **1973**, *70*, 2853.
(14) Birge, R. R.; Cooper, T. M. *Biophys. J.* **1983**, *42*, 61−69.
(15) Mathies, R. A.; Cruz, C. H. B.; Pollard, W. T.; Shank, C. V. *Science* **1988**, *240*, 777−779.
(16) Oesterhelt, D.; Tittor, J.; Bamberg, E. J. *Bioenerg. Biomemb.* **1992**, *24*, 181−191.
(17) Birge, R. R. *Nature* **1994**, *371*, 659.
(18) Patzelt, H.; Ulrich, A. S.; Egbringhoff, H.; Dux, P.; Ashurst, J.; Simon, B.; Oschkinat, H.; Oesterhelt, D. *J. Biomol. NMR* **1997**, *10*, 95−106.
(19) Rousso, I.; Khachatryanm E.; Gat, Y.; Brodsky, I.; Ottolenghi, M.; Sheves, M.; Lewis, A. *Proc. Natl. Acad. Sci. U.S.A.* **1997**, *94*, 7937−7941.
(20) Zhong, Q.; Ruhman, S.; Ottolenghi, M.; Sheves, M.; Friedman, N.; Atkinson, G. H.; Delaney, J. K. *J. Am. Chem. Soc.* **1996**, *118*, 12828−12829.
(21) Logunov, S. L.; Masciangioli, T. M.; Kamalov, V. F.; El-Sayed, M. A. *J. Phys. Chem. B* **1998**, *102*, 2303−2306.
(22) Pogozheva, I. D.; Lomize, A. L.; Mosberg, H. I. *Biophys. J.* **1997**, *72*, 1963−1985.
(23) Edholm, O.; Berger, O.; Jähnig, F. *J. Mol. Biol.* **1995**, *250*, 94−111.
(24) Humphrey, W.; Logunov, I.; Schulten, K.; Sheves, M. *Biochemistry* **1994**, *33*, 3668−3678.
(25) Humphrey, W.; Xu, D.; Sheves, M.; Schulten, K. *J. Phys. Chem.* **1995**, *99*, 14549−14560.
(26) Logunov, I.; Humphrey, W.; Schulten, K.; Sheves, M. *Biophys. J.* **1995**, *68*, 1270−1282.
(27) Logunov, I.; Schulten, K. *J. Am. Chem. Soc.* **1996**, *118*, 9727−9735.
(28) Humphrey, W.; Lu, H.; Logunov, I.; Werner, H.-J.; Schulten, K. *Biophys. J.* **1998**, *75*, 1689−1699.
(29) Warshel, A. *Nature* **1976**, *260*, 679−683.
(30) Warshel, A.; Barboy N. *J. Am. Chem. Soc.* **1982**, *104*, 1469−1476.
(31) Warshel, A.; Chu Z. T.; Hwang, J.-K. *Chem. Phys.* **1991**, *158*, 303−314.
(32) Grossjean, M. F.; Tavan, P. *J. Chem. Phys.* **1988**, *88*, 4884−4896.
(33) Tavan, P.; Schulten, K.; Oesterhelt, D. *Biophys. J.* **1985**, *47*, 415−430.
(34) Birge, R. R.; Schulten, K.; Karplus, M. *Chem. Phys. Lett.* **1975**, *31*, 451−454.
(35) Schulten, K.; Dinur, U.; Honig, B. *J. Chem. Phys.* **1980**, *73*, 3927−3935.
(36) Kurihara, Y.; Aoki; Y.; Imamura, A. *J. Chem. Phys.* **1997**, *107*, 3569−3575.
(37) Birge, R. R.; Hubbard, L. M. *Biophys. J.* **1981**, *34*, 517−134.
(38) Birge, R. R.; Murray, L. P.; Zidovetzki, R.; Knapp, H. M. *J. Am. Chem. Soc.* **1987**, *109*, 2090−2101.
(39) Tallent, J. R.; Hyde, E. W.; Findsen, L. A.; Fox, G. C.; Birge, R. R. *J. Am. Chem. Soc.* **1992**, *114*, 1581−1592.
(40) Tallent, J. R.; Birge, J. R.; Zhang, C.-F.; Wenderholm, E.; Birge, R. R. *Photochem. Photobiol.* **1992**, *56*, 935−952.
(41) Sakai, K.; Vacek, G.; Lüthi, H. P.; Nagashima, U. *Photochem. Photobiol.* **1997**, *66*, 532−540.

10.1021/ja983708a CCC: $18.00
Published on Web 12/11/1999

models. The bibliography is huge and not exhausted by the references cited here. Still, the understanding of the dynamics of these photoreactions remains an open problem in photochemistry and biology (see, e.g. refs 19 and 20). In particular, first principles calculations could greatly contribute to create an accurate picture of the rhodopsin photoreaction. Unfortunately, applying sophisticated methods to the excited state of such a complex system is very difficult. Hence, *ab initio* methods have been mainly applied to the ground state. The *ab initio* calculations for the excited states usually use simplified models;[28,43−51] in the few excited-state calculations for the whole chromophore, geometries were not optimized.[53−55]

To gain insight into the microscopic details of rhodopsin photoisomerization, we have applied a recently developed computational method that allows us to perform from first principles, within a variational density functional theory scheme, both structural relaxations and molecular dynamics simulations in the first excited singlet state.[63] With this relatively simple approach, inspired by the Ziegler−Rauk−Baerends sum method[64] and by the restricted open shell Hartree−Fock method,[65] the excited state geometries and energies of fairly large systems (up to hundred atoms) can be investigated, with an efficiency comparable to the well-established density functional theory treatment of the ground state.[66] The electronic excitation is modeled by transferring a single electron to an unoccupied orbital: this means that a HOMO−LUMO single excitation is pre-assumed. Electron correlation effects are included *via* the exchange and correlation potential rather then by using many determinants. The method has been tested on a series of small unsaturated compounds, by calculating energies and geometries for both vertical and adiabatic excitations. The results show a reasonable accuracy compared to experiments and more sophisticated multireference calculations. As with time-dependent density functional theory calculations, the excitation energies are underestimated. However, since an essentially constant energy shift is found for both vertical and adiabatic excitation energies, the shape of the potential energy surfaces should not be much affected and the resulting molecular dynamics should be reasonably accurate: this has been confirmed by a molecular dynamics simulation of the *cis*−*trans* isomerization process of formaldimine.[63] The formalism has been developed for a nondegenerate S_1 state, but it can be extended to other symmetries. This method has proved to work reasonably well in cases where the transition to the lowest excited state is known to be quite a pure HOMO−LUMO transition.[63] In rhodopsin the situation may be much more complex, and our technique too simplified to give an appropriate description. However, we hope that the additional information, provided by our method, on structural relaxations in the excited state can offer some valuable insights into the photoisomerization process. In refs 67−69 an analogous scheme and some applications are presented; problems associated with the use of approximate density functionals and perspectives are also discussed, providing further elements for evaluating the method. Improvements of the method might be possible, but while they would lead to more accurate results, in general they would also increase the computational workload, hindering the relaxation of excited state geometries for systems of relatively large size, which is our present goal.

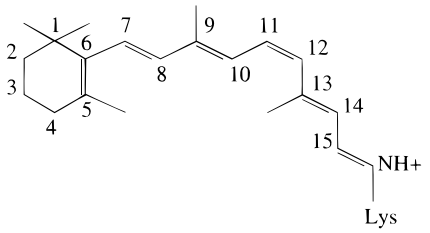

Figure 1. Sketch of the 11-*cis* isomer of the rhodopsin protein with the conventional numbering of the carbon atoms. The linkage *via* the protonated Schiff base to the protein through the lysine amino acid is shown.

In this paper, we present a series of calculations for the energetic and structural changes that the rhodopsin chromophore undergoes as it isomerizes from *cis* to *trans*. Various chromophore models of increasing complexity, including, in turn, the protonated Schiff base linkage and some relevant parts of the protein environment, were considered (see Figure 2). In all cases, the chromophore was modeled in an orthorombic cell of size 21.17 × 11.64 × 11.64 Å^3. No periodic images of the system were involved in the calculations.[70] We used the gradient-corrected functional proposed by Becke, Lee, Yang, and Parr (BLYP)[71,72] and Troullier-Martins norm-conserving

(42) Locknar, S. A.; Peteanu, L. A. *J. Phys. Chem. B* **1998**, *102*, 4240−4246.
(43) Dobado, J. A.; Nonella, M. *J. Phys. Chem.* **1996**, *100*, 18282−18288.
(44) Vreven, T.; Bernardi, F.; Garavelli, M.; Olivucci, M.; Robb, M. A.; Schlegel H. B. *J. Am. Chem. Soc.* **1997**, *119*, 12687−12688.
(45) Garavelli, M.; Celani, P.; Bernardi, F.; Robb, M. A.; Olivucci, M. *J. Am. Chem. Soc.* **1997**, *119*, 6891−6901.
(46) Garavelli, M.; Bernardi, F.; Olivucci, M.; Vreven, T.; Klein, S.; Celani, P.; Robb, M. A. *Faraday Discuss.* **1998**, *110*, 51−70.
(47) Garavelli, M.; Bernardi, F.; Celani, P.; Robb, M. A.; Olivucci, M. *J. Photochem. Photobiol. A* **1998**, *114*, 109−116.
(48) Garavelli, M.; Vreven, T.; Celani, P.; Bernardi, F.; Robb, M. A.; Olivucci, M. *J. Am. Chem. Soc.* **1998**, *120*, 1285−1288.
(49) Garavelli, M.; Negri, F.; Olivucci, M. *J. Am. Chem. Soc.* **1999**, *121*, 1023−1029.
(50) Garavelli, M.; Bernardi, F.; Robb, M. A.; Olivucci, M. *J. Mol. Struct. (THEOCHEM)* **1999**, *463*, 59−64.
(51) Martin, C. H. *J. Phys. Chem.* **1996**, *100*, 14310−14315.
(52) Du, P.; Davidson, E. R. *J. Phys. Chem.* **1990**, *94*, 7013−7020.
(53) Merchán, M.; Gonzáles-Luque, R. *J. Chem. Phys.* **1997**, *106*, 1112−1122.
(54) Yamamoto, S.; Wasada, H.; Kakitani, K. *J. Mol. Struct. (THEOCHEM)* **1998**, *451*, 151−162.
(55) Yamamoto, S.; Wasada, H.; Kakitani, K. *J. Mol. Struct. (THEOCHEM)* **1999**, *462*, 463−471.
(56) Terstegen, F.; Buss, V. *Chem. Phys.* **1997**, *225*, 163−171.
(57) Bifone, A.; de Groot, H. J. M.; Buda, F. *Chem. Phys. Lett.* **1996**, *248*, 165−172.
(58) Buda, F.; de Groot, H. J. M.; Bifone, A. *Phys. Rev. Lett.* **1996**, *77*, 5405−5408.
(59) Bifone, A.; de Groot, H. J. M.; Buda, F. *J. Chem. Phys. B* **1997**, *101*, 2954−2958.
(60) Bifone, A.; de Groot, H. J. M.; Buda, F. *Pure Appl. Chem.* **1997**, *69*, 2105−2110.
(61) La Penna, G.; Buda, F.; Bifone, A.; de Groot, H. J. M. *Chem. Phys. Lett.* **1998**, *294*, 447−453.
(62) Beppu, Y.; Kakitani, T.; Tokunaga, F. *Photochem. Photobiol.* **1992**, *56*, 1113−1117.
(63) Frank, I.; Hutter, J.; Marx, D.; Parrinello, M. *J. Chem. Phys.* **1998**, *108*, 4060−4069.
(64) Ziegler, T.; Rauk, A.; Baerends, E. J. *Theor. Chim. Acta* **1977**, *43*, 261.
(65) Roothaan, C. C. J. *Rev. Mod. Phys.* **1960**, *32*, 179.
(66) Parrinello, M. *Solid State Communications* **1997**, *102*, 107−120. Galli, G.; Parrinello, M. In *Computer Simulations in Materials Science*; Pontikis, V., Meyer, M., Eds.; Kluwer: Dordrecht, 1991. Payne, M. C.; Teter, M. P.; Allan, D. C.; Arias, T. A.; Joannopoulos, J. D. *Rev. Mod. Phys.* **1992**, *64*, 1045−1097. Galli, G.; Pasquarello, A. In *Computer Simulations in Chemical Physics*; Allen, M. P., Tildesley, D. J., Eds.; Kluwer: Dordrecht, 1993.
(67) Filatov, M.; Shaik, S. *Chem. Phys. Lett.* **1998**, *288*, 689−697.
(68) Filatov, M.; Shaik, S. *J. Chem. Phys.* **1999**, *110*, 116−125.
(69) Filatov, M.; Shaik, S. *Chem. Phys. Lett.* **1999**, *304*, 429−437.
(70) Hockney, R. W. *Methods Comput. Phys.* **1970**, *9*, 136. Barnett, R. N.; Landman, U. *Phys. Rev. B* **1993**, *48*, 2081−2087.
(71) Becke, A. D. *Phys. Rev. A* **1988**, *38*, 3098−3100.
(72) Lee, C.; Yang, W.; Parr, R. C. *Phys. Rev. B* **1988**, *37*, 785−789.

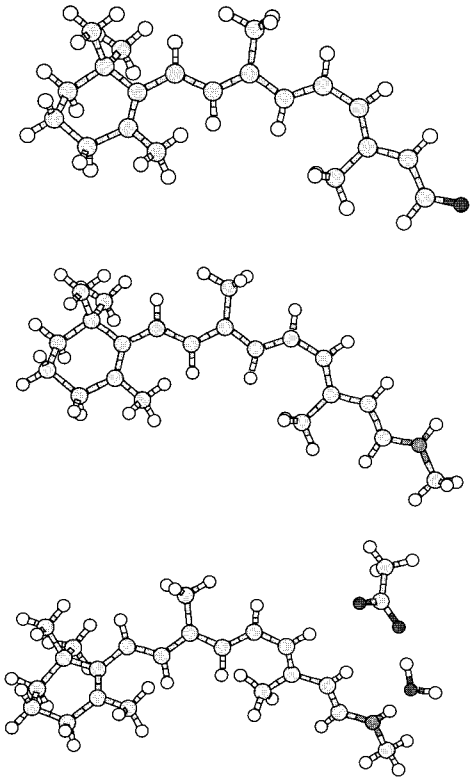

Figure 2. Models of the rhodopsin chromophore of increasing complexity used for the calculations: retinal (top panel); the protonated Schiff base of retinal (central panel); the protonated Schiff base of retinal with a counterionic group and a water molecule (bottom panel).

pseudopotentials.[73] The electronic wave functions were expanded in a plane wave basis set, with a kinetic energy cutoff of 70 Ry. To monitor the chromophore during the isomerization, we took the $C_{10}-C_{11}-C_{12}-C_{13}$ torsional angle (τ) to be the reaction coordinate; this angle was, in turn, constrained at values between $-180°$ and $180°$: $\tau \sim 0°$ corresponds to the ideal *cis* isomer, and $\tau \sim 180°$ to the *trans* one. Rotation and translation of the molecule in the simulation cell were frozen out by a set of constraints; all other structural degrees of freedom were fully relaxed.

The potential energy curves along the reaction path for the ground (S_0) and first excited singlet state (S_1) of the protonated Schiff base of retinal (Figure 2, central panel) are shown in Figure 3. These calculations were performed for the positively charged system without including any counterion. The isomerization process from *cis* to *trans* shows a large energy barrier, not only in the ground state (17 kcal/mol for $\tau \sim -90°$ and 21 kcal/mol for $\tau \sim 90°$), as expected, but also in the excited state (14 kcal/mol for $\tau \sim -90°$ and 16 kcal/mol for $\tau \sim 90°$). The S_1 energy barrier is clearly in disagreement with experiments,[5] which report a very fast and efficient photoisomerization. The slight asymmetry of the energy profile for positive and negative torsional angles is due to the nonplanarity of the β-ionone ring, which lowers the symmetry of the molecule. The calculations were performed using spin-unpolarized density functional theory; we have verified, by using the spin-polarized local spin density[74] approximation, that in the S_0 transition state no spin-unpairing takes place and that the energy barrier remains unchanged. We find that the energy of the *trans* isomer is lower than the *cis* energy, as usual for systems with unstrained double

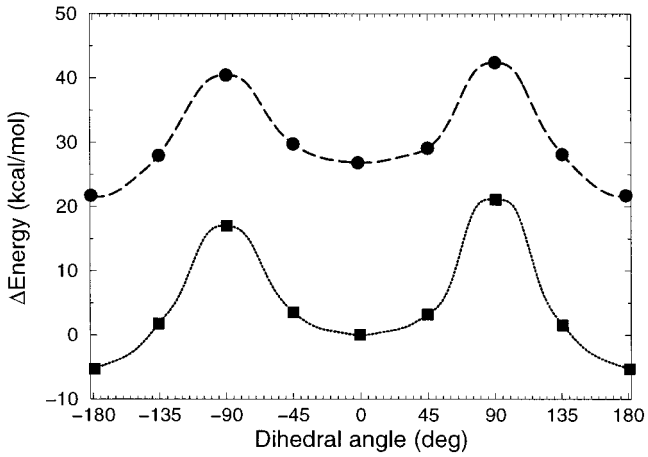

Figure 3. S_0 (squares) and S_1 (circles) energies, with respect to the ground state energy of the *cis* structure, as a function of the $C_{10}-C_{11}-C_{12}-C_{13}$ torsional angle for the protonated Schiff base of retinal in vacuum.

bonds. This is in contrast to experiments for the protein which show that the *cis* isomer is more stable by as much as 35 kcal/mol.[75] However, it must be observed that ours are gas-phase calculations that do not include any effect of the environment; in reality the final chromophore state is expected to be strained since it sits in a pocket designed for the *cis* isomer.[30]

A characteristic feature of systems with conjugated double bonds is the bond alternation between single and double bonds; the bond lengths can be directly related to the bond stabilities and rotational barriers: the shorter the bond, the higher is the barrier for the rotation about this bond. In Figure 4 we monitor the C−C bond lengths of the conjugated π-system for a set of structures of the protonated Schiff base of retinal along the reaction path (filled symbols). For comparison, we also show in the top panel of Figure 4 the C−C bond lengths for the unprotonated Schiff base of retinal (empty symbols): it is clear that the protonation of the Schiff base has a marked effect on the bond alternation. In the ground state, the alternation of single and double bonds typical of π-conjugated systems is recognizable for both *cis* and *trans* structures; the alternation is clearly reduced due to the protonation of the Schiff base linkage.[41] When the isomerization is forced by constraining the torsional angle about the $C_{11}-C_{12}$ bond, the $C_{11}-C_{12}$ bond increases in length, completely losing its original double bond character, which is finally regained in the *trans* form. For the structures with maximal energies the C−C bond pattern is distorted, especially in proximity to the $C_{11}-C_{12}$ bond. The main structural effect of the excitation consists of shortening the long bonds and lengthening the short bonds; these variations become smaller close to the protonated Schiff base linkage. We notice that the $C_{11}-C_{12}$ bond does not show any peculiarity with respect to the others: there seems to be no reason why, in the isolated chromophore, photoexcitation should lead to a predominant torsion about this particular bond. All the torsional angles in the chain of the conjugated double bonds, with the exception of course of the constrained $C_{10}-C_{11}-C_{12}-C_{13}$ one, have values very close to 180°, with the largest deviation shown by the $C_{11}-C_{12}-C_{13}-C_{14}$ angle in the maximum energy ground state structure. Because of the S_1 energy barrier, a molecular dynamics simulation of the protonated Schiff base of retinal would not result in any *cis*−*trans* isomerization on a time scale of some hundred femtoseconds. To check the stability of the investigated model with respect to any other possible reaction coordinate,

(73) Troullier, N.; Martins, J. L. *Phys. Rev. B* **1991**, *43*, 1993−2006.
(74) Gunnarsson, O.; Lundqvist, B. I. *Phys. Rev. B* **1976**, *13*, 4274−4298.
(75) Cooper, A. *Nature* **1979**, *282*, 531−533.

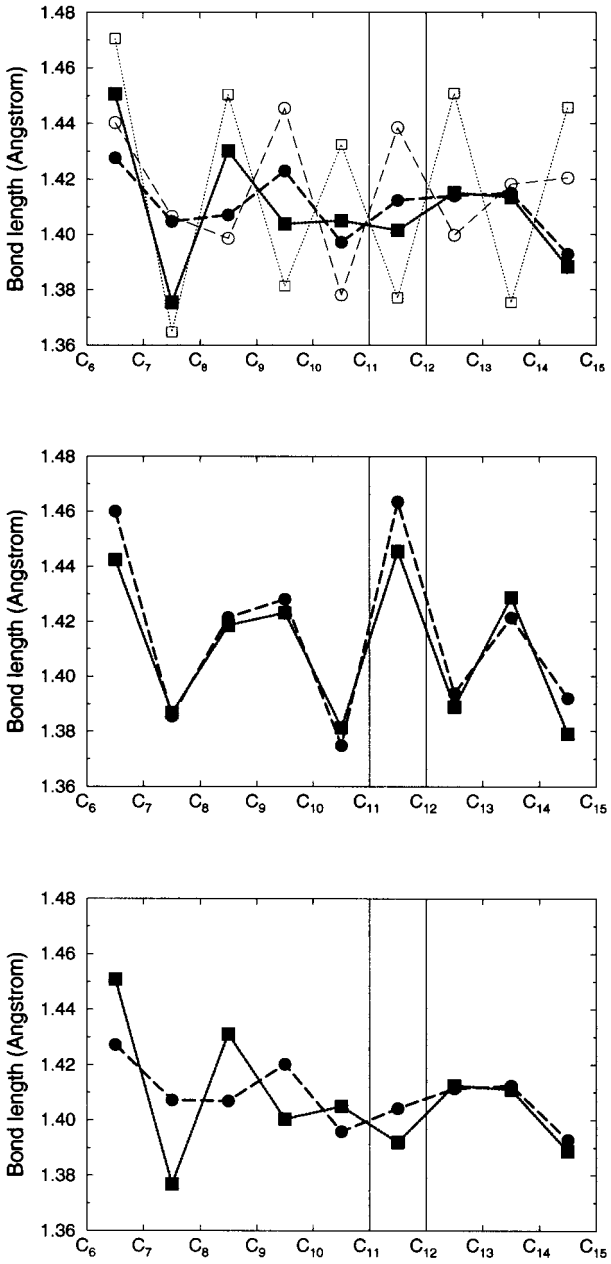

Figure 4. C−C bond lengths for the protonated Schiff base of retinal in the ground (filled squares) and excited (filled circles) states: $C_{10}-C_{11}-C_{12}-C_{13}$ ~0° (top panel), ~90° (central panel), and ~180° (bottom panel). The two vertical lines mark the $C_{11}-C_{12}$ bond involved in the photoisomerization. The C−C bond lengths for the unprotonated Schiff base of retinal in the *cis* configuration in the ground (empty squares) and excited (empty circles) states are also shown (top panel).

we have performed a molecular dynamics simulation of the protonated Schiff base of retinal at room temperature for about 480 fs in the ground state and for a further 270 fs in the excited state. No isomerization was observed; however, we found the system to be rather floppy: the variations of the torsional angle τ ranged from −42° to 16° in the ground state and from −43° to 11° in the excited state, with average values of −10° and −8°, respectively. The variations of the $C_{11}-C_{12}$ bond length were in the range of 1.34−1.47 Å in the ground state and of 1.35−1.46 Å in the excited state, with average values of 1.40 and 1.41 Å, respectively.

The energy barriers for both the $C_{13}-C_{14}$ isomerization and the $C_{11}-C_{12}$ isomerization of the very similar protonated chromophore of bacteriorhodopsin have been recently calculated

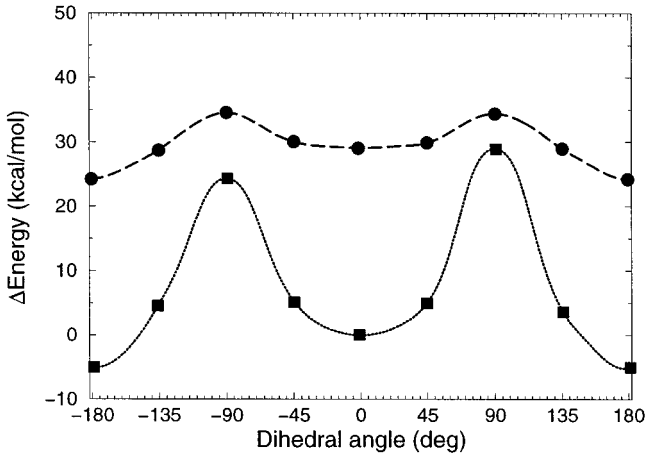

Figure 5. S_0 (squares) and S_1 (circles) energies, with respect to the ground state energy of the *cis* structure, as a function of the $C_{10}-C_{11}-C_{12}-C_{13}$ torsional angle for retinal in vacuum.

within the sa-CASSCF scheme.[54,55] Among the many calculations in the literature, these are the ones more directly comparable, for size of the systems and first principles character of the method, to our results. The sa-CASSCF results are qualitatively different from ours, and somehow more compatible with the experimental evidence: a small barrier is found for the isomerization in the excited state, and the S_1 potential energy curve shows a minimum at 90°. Of course, the difference with respect to our calculations can be due to the shortcomings of our method. However, the fact that in the sa-CASSCF calculations only part of the π electrons could be included into the active space and that the structures were not relaxed in the excited state might have considerable influence on the results. In fact, due to the use of a fixed geometry, the authors could present only part of the potential surface for the $C_{11}-C_{12}$ isomerization.

To analyze the influence of the protonation on the properties of the system, we have also investigated the S_0 and S_1 energy curves of the free retinal chromophore, i.e. without the protonated Schiff base linkage (Figure 2, top panel). We found ground-state barriers for the *cis* to *trans* isomerization of 24 ($\tau \sim -90°$) and 29 kcal/mol ($\tau \sim 90°$), comparable to those of the protonated Schiff base. However, in the excited state the barriers are much lower: 5 kcal/mol for both $\tau \sim -90°$ and $\tau \sim 90°$ (see Figure 5). In Figure 6, the C−C bond lengths for the ground and excited states of retinal are shown. In the ground state the *cis* and *trans* isomers show a clear alternation of single and double bonds (Figure 6, top and bottom panels), not affected by the presence of a charge at the end of the chain as in the case of the protonated Schiff base. This alternation is maintained to a good degree even in the structure corresponding to the maximum energies (Figure 6, central panel). Again the effect of the excitation is to lengthen the short bonds and shorten the long ones. In this case, for the *cis* and *trans* isomers, the alternation of the bond length in the central part of the C−C chain is basically reversed, thus lowering the barrier for the excited state double bond isomerization. The energy barriers for the $C_{11}-C_{12}$ isomerization of retinal have been studied using multiconfigurational second-order perturbation theory through the CASPT2 formalism;[53] although these calculations are not quantitatively comparable to ours since their excited state structures were not relaxed, they show very similar trends, with a lower energy for the *trans* isomer than for the *cis* isomer, and barriers in both the ground and the first excited singlet state.

There are several possible explanations for the inconsistencies between our results for the excited state barrier of the protonated

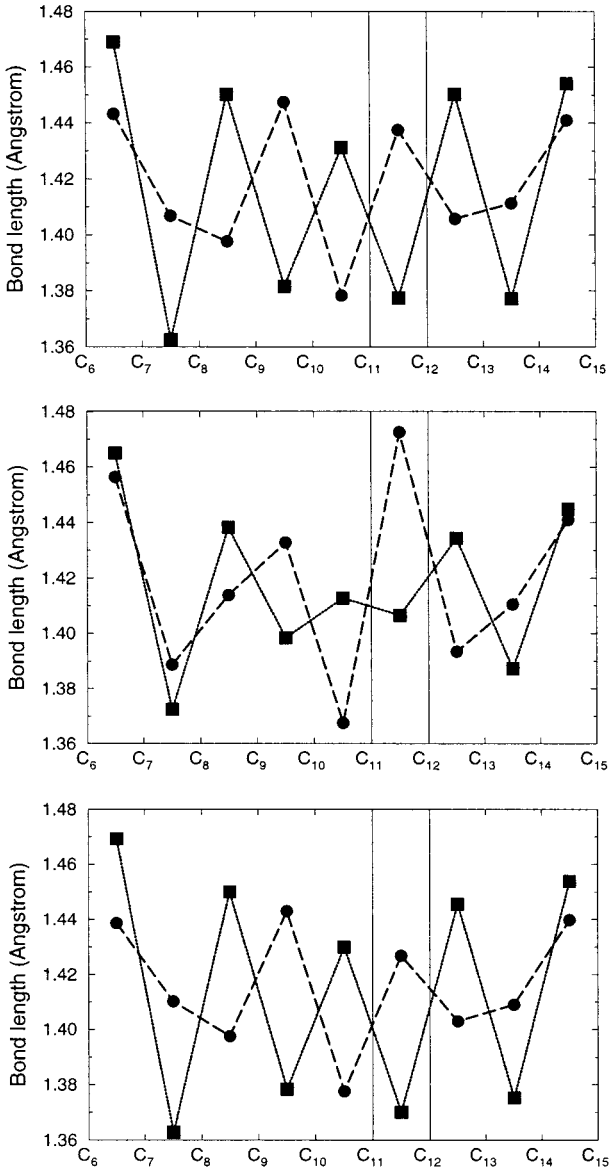

Figure 6. C−C bond lengths for retinal in the ground (filled squares) and excited (filled circles) states: $C_{10}-C_{11}-C_{12}-C_{13}$ ~0° (top panel), ~90° (central panel), and ~180° (bottom panel). The two vertical lines mark the $C_{11}-C_{12}$ bond involved in the photoisomerization.

Schiff base of retinal and the experimental evidence for the photoisomerization of rhodopsin. Our method has some limitations: it is restricted to a HOMO−LUMO excitation and we use an exchange-correlation energy functional which has been developed for the ground and not for the excited state and that in any case is approximate. We did not try to investigate, using, e.g., a surface hopping algorithm,[76] the effect of nonadiabaticity which should be involved at some stage of the reaction (see, e.g., refs 28, 39, 44, and 77): the inclusion of nonadiabatic effects would make our scheme computationally more expensive and at present we are mainly interested in keeping the method as simple as possible to be able to treat relatively complex systems. Furthermore, our method does not deal with double excitations that might become important during the isomerization process, as suggested by semiempirical calculations,[32,34,35] and induce a reordering of the excited states.[78] If this is the case, our calculations would not describe the state that is relevant to the isomerization but rather a higher one. Yet, the importance of explicitly including double excitations within a density functional theory based method is unclear; in fact for other systems it has been found that double excitation effects are to some extent accounted for by the density functional treatment, at variance from conventional Hartree−Fock based configuration interaction schemes.[79,80] For the case of rhodopsin no unique answer can be obtained from the literature. In principle multiconfiguration SCF methods can help us to understand how important double excitations are for the protonated Schiff base isomerization. In the recent sa-CASSCF study of the $C_{11}-C_{12}$ isomerization[55] there is no indication for a significant double excitation character of the S_1 state. However, the possibility of a relevant influence of double excitations on the shape of the S_1 potential energy surface cannot be excluded on the basis of the data provided in ref 55.

In the present study we concentrate on another possible reason for deviations from experiment: we are in fact considering the chromophore in isolation, without taking into account any interaction with the protein. The protein environment should strongly influence the details of the photoreaction, the isomerization pathway, and the quantum yield: this is evident from the different behaviors of rhodopsin and bacteriorhodopsin, of the chromophore in solution[81−83] and in the protein, and by the results of mutagenesis experiments.[87] The chromophore photoisomerization is catalyzed by the protein environment; in solution it is much slower and it has been concluded that there is an energy barrier in the excited state.[82] The importance of the environment has also been shown previously by theoretical investigations, see e.g. refs 27, 28, and 31−33, by including charges or residues close to the chromophore or even modeling the whole protein. Here we try to assess the influence of the protein environment on the photoisomerization barriers and on the chromophore structure within our computational scheme.

Some clues of the importance of the environment effects can be found in Figure 7, where the dipole moments, calculated with respect to the center of the ion core charges, of the isolated Schiff base of retinal for the ground and excited state structures are shown. While in the *cis* and *trans* conformations the dipole moments for both states are similar, they show an opposite trend in the transition state structures, decreasing in the ground state and increasing in the excited state. This behavior suggests that, along the reaction path, the chromophore would interact with the protein differently in the ground than in the excited state: thus the S_0 and S_1 isomerization barriers are likely to change in opposite directions. The dipole moments of retinal (also in Figure 7) and of the unprotonated Schiff base show a different behavior: upon excitation they increase with respect to the initial ground-state value, then decrease at 90° and increase again at 180°; in the ground state a maximum at 90° was found: the dipole moment variations are much smaller than in the protonated Schiff base. The available experimental data[42,84−86] are

(76) Coker, D. F. Computer simulation methods for nonadiabatic dynamics in condensed systems. In *Computer Simulation in Chemical Physics*; Allen, M. P., Tildesley, D. J., Eds.; Kluwer: Academic: Dordrecht, 1993.

(77) Ben-Nun, M.; Molnar, F.; Lu, H.; Phillips, J. C.; Martinez, T. J.; Schulten, K. *Faraday Discuss.* **1998**, *110*, 447−462.

(78) Hudson, B.; Kohler, B. *Annu. Rev. Phys. Chem.* **1974**, *25*, 437−460.

(79) Grimme, S. *Chem. Phys. Lett.* **1996**, *259*, 128−137.

(80) Hirata, S.; Head-Gordon, M. *Chem. Phys. Lett.* **1999**, *302*, 375−382.

(81) Hamm, P.; Zurek, M.; Röschinger, T.; Patzelt, H.; Oesterhelt, D.; Zinth, W. *Chem. Phys. Lett.* **1996**, *263*, 613−621.

(82) Logunov, S. L.; Song, L.; El-Sayed, M. A. *J. Phys. Chem.* **1996**, *100*, 18586−18591.

(83) Kandori, H.; Katsuta, Y.; Masayoshi, I.; Sasabe, Hiroyuki *J. Am. Chem. Soc.* **1995**, *117*, 2669−2670.

(84) Mathies, R.; Stryer, L. *Proc. Natl. Acad. Sci. U.S.A.* **1976**, *73*, 2169−2173.

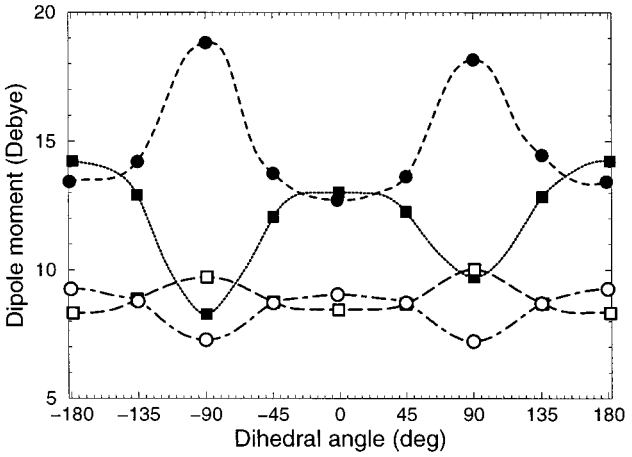

Figure 7. Dipole moments for the protonated Schiff base of retinal (filled symbols) and for retinal (empty symbols) in the S_0 (squares) and S_1 (circles) states as a function of the $C_{10}-C_{11}-C_{12}-C_{13}$ torsional angle.

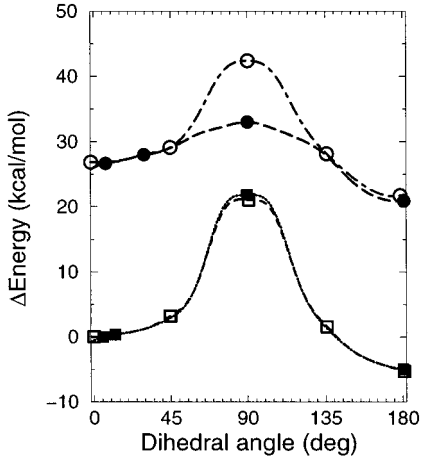

Figure 8. S_0 (squares) and S_1 (circles) energies, with respect to the ground state energy of the *cis* structure, as a function of the $C_{10}-C_{11}-C_{12}-C_{13}$ torsional angle for the protonated Schiff base of retinal with (filled symbols) and without (empty symbols) the counterion group and the water molecule.

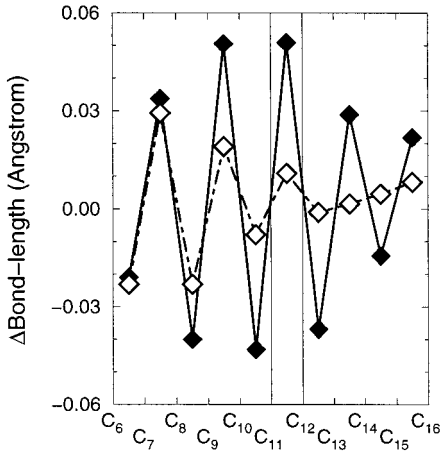

Figure 9. The difference in the C−C and C−N bond lengths between the S_1 and S_0 *cis* structures for the protonated Schiff base of retinal with (filled symbols) and without (empty symbols) the counterion group and the water molecule.

for retinal, the unprotonated Schiff base, and a Cl^- salt of the protonated Schiff base in *all-trans* and various *cis* configurations, in solution or in plastic films. They measured a remarkable increment of the dipole moment upon excitation. Examples of values of $\Delta\mu$ found for *all-trans* retinal include ∼12.2,[42] ∼15.6,[84] and ∼13.2 D;[85] extrapolated values, which should be considered with caution, indicate that in the gas phase the increment should be smaller than in the condensed phase ($\Delta\mu$ ∼ 1.7 D in ref 85). In fact for *all-trans* retinal we found a ground state dipole moment of 8.3 D that increases to 9.3 D upon adiabatic excitation (9.8 D upon vertical excitation). In the case of the unprotonated Schiff base the calculated ground state dipole moment was 3.4 D, lower than in retinal and in the protonated Schiff base, increasing to 4.0 D upon adiabatic excitation.

Even with state-of-the-art codes and computers, we cannot model the whole protein from first principles. Nevertheless, as a first approximation, we can include some relevant parts of the protein close to the chromophore. Since the chromophore is charged, the most important interaction should be that with a counterionic group, which has been identified as glutamate and localized with respect to the chromophore.[88−93] It has been suggested that such an interaction is bridged by a water molecule that forms hydrogen bonds with both the glutamate and the protonated Schiff base.[92−94] We have therefore included the side chain of the glutamate amino acid as a counterion plus a water molecule to mediate the interaction (see Figure 2, bottom panel), located as suggested in the model of ref 22 for the initial *cis* isomer. We prepared a set of structures with different values of τ, but fixed relative orientations of the glutamate, the water molecule, and the N−H group of the Schiff base; each structure was then allowed to relax under the condition of constant τ. Such an arrangement was found to be stable for all values of the torsional angle τ. The S_0 and S_1 potential energy curves for positive values of the torsion angle τ are shown in Figure 8. While in the ground state the barrier is slightly larger than in the absence of the counterion (22 kcal/mol vs 21 kcal/mol), in the excited state it is markedly lower (6 kcal/mol vs 16 kcal/mol). The photoisomerization in this model system is still not barrierless, but these results clearly show the importance of the interactions with the environment. The presence of the counterion somehow neutralizes the effect of the Schiff base proton, restoring a behavior similar to that found in the neutral system, with the alternation of the single and double bonds reversed upon excitation. The effects of the counterion become evident upon analyzing the variation in the C−C bond length upon excitation (Figure 9). In particular the $C_{11}-C_{12}$ double bond undergoes a remarkable change, to become a favorite candidate for the isomerization.

In summary, by performing, within a density functional theory based scheme, total energy calculations of the S_0 and S_1 potential energy curves for the protonated Schiff base of retinal we have observed a high energy barrier for the photoisomerization from *11-cis* to *all-trans*. This barrier is substantially reduced by the interaction with a counterionic group, which was modeled by

(85) Ponder, M.; Mathies, R. *J. Phys. Chem.* **1983**, 5090−5098.
(86) Corsetti, J. P.; Koher, B. E. *J. Phys. Chem.* **1977**, *67*, 5237−5243.
(87) Song, L.; El-Sayed, M. A.; Lanyi, J. K. *Science* **1993**, *261*, 891−894.
(88) Sakmar, T.; Franke, R.; Khorana, G. *Proc. Natl. Acad. Sci. U.S.A.* **1989**, *86*, 8309−8313.
(89) Jäger, F.; Fahmy, K.; Sakmar, T. P.; Siebert, F. *Biochemistry* **1994**, *33*, 10878−10882.
(90) Zhukovsky, E.; Oprian, D. *Science* **1989**, *246*, 928−930.
(91) Han, M.; Dedecker, B. S.; Smith, S. O. *Biophys. J.* **1993**, *65*, 899−906.
(92) Han, M.; Smith, S. O. *Biochemistry* **1995**, *34*, 1425−1432.
(93) Han, M.; Smith, S. O. *Biophys. Chem.* **1995**, *56*, 23−29.
(94) Deng, H.; Huang, L. W.; Callender, R.; Ebrey, T. *Biophys. J.* **1994**, *66*, 1129−1136.

the side chain of a glutamate amino acid and by a water molecule. Our results confirm that the protein environment has a strong influence on the photoisomerization.

We are aware that with our approach we have not provided a convincing picture of the rhodopsin photoisomerization. This could be due to the limitations of our method as discussed above, and/ or to the oversimplified model of the protein environment. However, we have demonstrated that it is indeed possible, by performing *ab initio* geometry optimizations, to monitor the structural changes that occur upon excitation for relatively complex systems such as the rhodopsin chromophore. These structural changes, which at present are not accessible to more sophisticated techniques, play an essential role in the photoisomerization process, as demonstrated by the correlation between the $C_{11}-C_{12}$ bond length and the corresponding torsional energy barrier. An improved but still simple *ab initio* scheme, providing both energies and relaxed geometries in the excited states, possibly in combination with a classical treatment of the protein environment, is therefore necessary to provide a better microscopic characterization of the rhodopsin photoreaction.

Acknowledgment. We thank Paolo Carloni [SISSA, Trieste, Italy] and Jürg Hutter [Max-Planck-Institut für Festkörperforschung, Stuttgart, Germany] for many useful discussions and suggestions.

JA983708A